Assessment of cardiac tumors by ^{18}F-FDG PET/CT imaging: Histological correlation and clinical outcomes

Jingjing Meng, MD,[a] Honglei Zhao, MD,[b] Yongmin Liu, MD,[b] Dong Chen, MD,[c] Marcus Hacker, MD,[d] Yongxiang Wei, MD, PhD,[a] Xiang Li, PhD,[a,d] Xiaoli Zhang, MD, PhD,[a] and Michael C. Kreissl, MD[e]

[a] Department of Nuclear Medicine, Laboratory for Molecular Imaging, Beijing Anzhen Hospital, Capital Medical University, Beijing, China
[b] Department of Cardiac Surgery, Beijing Anzhen Hospital, Capital Medical University, Beijing, China
[c] Department of Pathology, Beijing Anzhen Hospital, Capital Medical University, Beijing, China
[d] Division of Nuclear Medicine, Department of Biomedical Imaging and Image-Guided Therapy, Medical University of Vienna, Vienna, Austria
[e] Division of Nuclear Medicine, Department of Radiology and Nuclear Medicine, University Hospital Magdeburg, Magdeburg, Germany

Received Oct 4, 2019; accepted Dec 15, 2019
doi:10.1007/s12350-019-02022-1

Background. **To evaluate the diagnostic value of ^{18}F-FDG PET/CT in distinguishing benign versus malignant cardiac tumors as well as to assess its prognostic value.**

Methods. **We analyzed 38 patients with cardiac tumors who underwent ^{18}F-FDG PET/CT and followed for median 8.5 ± 12.5 months. SUV_{max} and TBR_{max} (maximum tumor-to-background ratio) by receiver-operating characteristic (ROC) curve analysis were used to obtain threshold for the diagnosis of malignancy as defined by histology (n = 38). Survival was assessed and correlated with the dignity of the lesions and PET parameters.**

Results. **Optimal cut-off values indicating malignancy were as follows: SUV_{max} = 3.44, with 100% sensitivity and 92.9% specificity, and TBR_{max} = 1.55, with 95.8% sensitivity and 92.9% specificity. A significant difference of ^{18}F-FDG uptake was observed between primary benign (n = 14, SUV_{max} = 2.35 ± 1.31, TBR_{max} = 1.05 ± 0.50) compared to primary malignant cardiac tumors (n = 11, SUV_{max} = 8.90 ± 4.23, TBR_{max} = 3.82 ± 1.44) as well as cardiac metastases and lymphoma (n = 13, SUV_{max} = 14.37 ± 8.05, TBR_{max} = 6.19 ± 3.38) (all $P < .001$). Survival rate was significantly lower in patients with malignant as compared to benign cardiac tumors ($P < .05$). Regression analysis revealed that the lesion dignity determined by the cut-off value of SUV_{max} was an independent predictor for death in patients with cardiac tumors ($P < .05$).**

Electronic supplementary material The online version of this article (https://doi.org/10.1007/s12350-019-02022-1) contains supplementary material, which is available to authorized users.

The authors of this article have provided a PowerPoint file, available for download at SpringerLink, which summarizes the contents of the paper and is free for re-use at meetings and presentations. Search for the article DOI on SpringerLink.com.

All editorial decisions for this article, including selection of reviewers and the final decision, were made by guest editor Nagara Tamaki, MD.

Funding This work was supported by National Natural Science Foundation of China [81071177, 81871377, 81571717] and Capital Characteristic Clinical Application Research [Z181100001718071].

Jingjing Meng and Xiang Li have contributed equally to the manuscript.

Reprint requests: Xiaoli Zhang, MD, PhD, Department of Nuclear Medicine, Laboratory for Molecular Imaging, Beijing Anzhen Hospital, Capital Medical University, No. 2 Anzhen Road, Chaoyang District, Beijing100029, China; *xlzhang68@126.com*

J Nucl Cardiol 2021;28:2233–43.
1071-3581/$34.00

Conclusion. **^{18}F-FDG uptake in cardiac tumors can differentiate between benign and malignant cardiac tumors and predicts survival. (J Nucl Cardiol 2021;28:2233–43.)**

Key Words: Cardiac tumor • ^{18}F-FDG • PET/CT • diagnosis • cardiac metastasis • prognosis

Abbreviations	
^{18}F-FDG	^{18}Fluorine-fluorodeoxyglucose
AUC	Area-under-the-curve
CMR	Cardiac magnetic resonance imaging
DLBCL	Diffuse large B-cell lymphoma
PET/CT	Positron emission tomography/computed tomography
PAS	Periodic acid-schiff
ROC	Receiver-operating characteristic
SUV_{max}	Maximum standardized uptake value
TBR_{max}	Maximum tumor-to-background ratio
VOI	Volume of interest

INTRODUCTION

With an incidence of only 0.0017% to 0.02%, primary cardiac tumors are rare;[1] however, cardiac metastases of extracardiac malignancies occur much more frequently.[2] For primary cardiac tumors, the likelihood of malignancy is reported between 20% and 25%.[3,4]

Primary cardiac tumors are mainly treated by surgical resection. Metastatic cardiac tumors in most cases are not referred to surgery; this especially applies to patients with cardiac manifestations of lymphoma,[5] which can be treated by chemotherapy and/or radiation therapy. Hence, a thorough initial staging is essential to the management of cardiac tumors in order to choose the best treatment strategy.

Noninvasive imaging plays an important role for the work-up of an undetermined cardiac masses, since percutaneous biopsy typically is not feasible, and surgical biopsy or resection carries a high risk of perioperative complications.[5,6] Echocardiography, cardiac magnetic resonance imaging (CMR) or computed tomography (CT), particularly with contrast enhancement, allow assessment of multiple morphologic features. In some instances, these modalities permit to diagnose a specific tumor type, e.g., myxoma.[7] Even though morphologic features can help to differentiate malignant from benign tumors,[8] individual morphological feature usually does not allow for a precise determination of dignity. Cardiac MR has a very high resolution; however, the duration of image acquisition can be fairly long. Also, its use is limited in patients with pacemakers or other metal implants.

^{18}F-fluorodeoxyglucose (^{18}F-FDG) PET/CT has become an essential tool in managing a variety of malignancies.[9-12] This modality provides noninvasive whole-body information and can also identify the most aggressive malignant lesion.[13] In many tumors, accurate diagnosis is nowadays essential for individual decision-making to decide on the right treatment strategy, and further, to improve patient's outcome. Nonetheless, to date, only a few studies, with a limited number of patients, have been published, which used ^{18}F-FDG PET/CT to differentiate benign from malignant cardiac tumors.[14,15] So far, the prognostic value of ^{18}F-FDG PET/CT in patients with cardiac tumors has not been reported.

This retrospective study aimed to evaluate the diagnostic value of ^{18}F-FDG PET/CT in the determination of the dignity of cardiac tumors with histopathology serving as the gold standard. Also, the prognostic value of ^{18}F-FDG PET/CT in patients with cardiac tumors was assessed.

MATERIALS AND METHODS

Study Population

Initially included in the analysis were 66 consecutive patients with cardiac tumors referred to Beijing Anzhen Hospital, China, from January 2015 to May 2019 for staging by whole-body ^{18}F-FDG PET/CT. 38 patients with available histopathology could be enrolled in current study (Figure 1). Electronic medical records were reviewed; this included clinical characteristics, symptoms, imaging findings by echocardiography, CT, cardiac MR (if available), histological results, and treatment strategy.

This analysis was approved by the Beijing Anzhen Hospital ethics committee and conducted according to the Helsinki Declaration. Patients provided written informed consent for the imaging procedures as well as for the participation in anonymized analyses such as this.

Patient Preparation and ^{18}F-FDG PET/CT

All patients underwent ^{18}F-FDG PET/CT imaging after a high-fat diet.[16] Additionally, they fasted for $\geq$ 12 h and had blood glucose $<$ 10 mmol/L before imaging. The average ^{18}F-FDG activity of 254 ± 67 MBq (6.9 ± 1.8 mCi), 5 MBq/kg (0.13 mCi/kg) of body weight was injected intravenously; radiation exposure for the combined PET/CT ranged from 11.6 to 17.8 mSv per patient per procedure.

Imaging was performed 60 min after ^{18}F-FDG injection, using a high-spatial-resolution, full-ring PET scanner (Biograph mCT, Siemens Healthcare, Erlangen, Germany). The imaging data were reconstructed using a point spread function and a time-of-flight algorithm (TrueX+time-of-flight, UltraHD-PET), with 2 iterations and 21 subsets. Subsequently, a Gaussian filter with 2 mm full-width half-maximum was applied to the reconstructed images. For attenuation and scatter correction, a CT without contrast agent was used. Here, slice thickness was 5 mm with a pitch of 0.8 and a tube voltage of 120 kV. The tube current automatically modulated according to the patient's size and body shape; a 210 mAs maximum reference value was used to achieve good image quality. Representative ^{18}F-FDG PET/CT images from the patient's collective are shown in Figures 2, 3, and 4.

Image Analysis

PET/CT datasets were reviewed and analyzed by two readers, both board-certified nuclear medicine physicians and PET/CT experts, to determine ^{18}F-FDG uptake of the cardiac tumors and to screen for extracardiac malignant manifestations by visual interpretation. The maximum standardized uptake value (SUV_{max}) was derived from a 3-dimensional volume of interest (VOI) assigned to the tumor. This VOI was placed within the tumor at the location of the highest tracer uptake. Caution was taken to exclude unspecific myocardial uptake from the analysis. In case of very low glucose metabolism, the coregistered CT data were used to help assign the VOI. In order to calculate the maximum tumor-to-background ratio (TBR_{max}), the SUV_{max} of each tumor was normalized by the mean SUV of a spherical reference VOI, 3 cm in diameter, assigned to the right lobe of the liver. If an extracardiac hypermetabolic lesion was verified as tumor by histology or biopsy and the ^{18}F-FDG uptake pattern was similar with the cardiac tumors, the cardiac tumors were deemed to be of the same entity.

Histological Analysis

Pathological materials from all patients studied were available for gross and histological examinations. Specimens were fixed in formalin, routinely processed for light microscopy and stained with hematoxylin-eosin, periodic acid-schiff (PAS), azan and Weigert van Gieson. Also, transmission electron microscopy and immunohistochemistry studies were performed to confirm the histological diagnosis. The results were confirmed by two experienced pathologists who were blinded to the previous clinical findings and location of the tumors. According to histological diagnosis,[17] the 38 patients were divided into three groups, Group 1 with primary benign cardiac tumor, Group 2 with primary malignant cardiac tumor, and Group 3 with cardiac metastases and lymphoma.

Follow-Up

Follow-up was performed by review of patients' clinical records and by phone contact with patients or their relatives. Thirty-eight patients were followed for 8.5 ± 12.6 months [median ± interquartile range (IQR) 25th to 75th percentiles], range 1-52 months. 13 patients (34.2%) died during follow-up.

Statistics

Data were analyzed using SPSS 19.0 (SPSS Inc. IBM, Armonk, NY). Continuous parametric variables were expressed as the mean ± standard deviation (SD). Non-parametric variables were displayed as the median ± IQR. The mean values of continuous variables were compared between

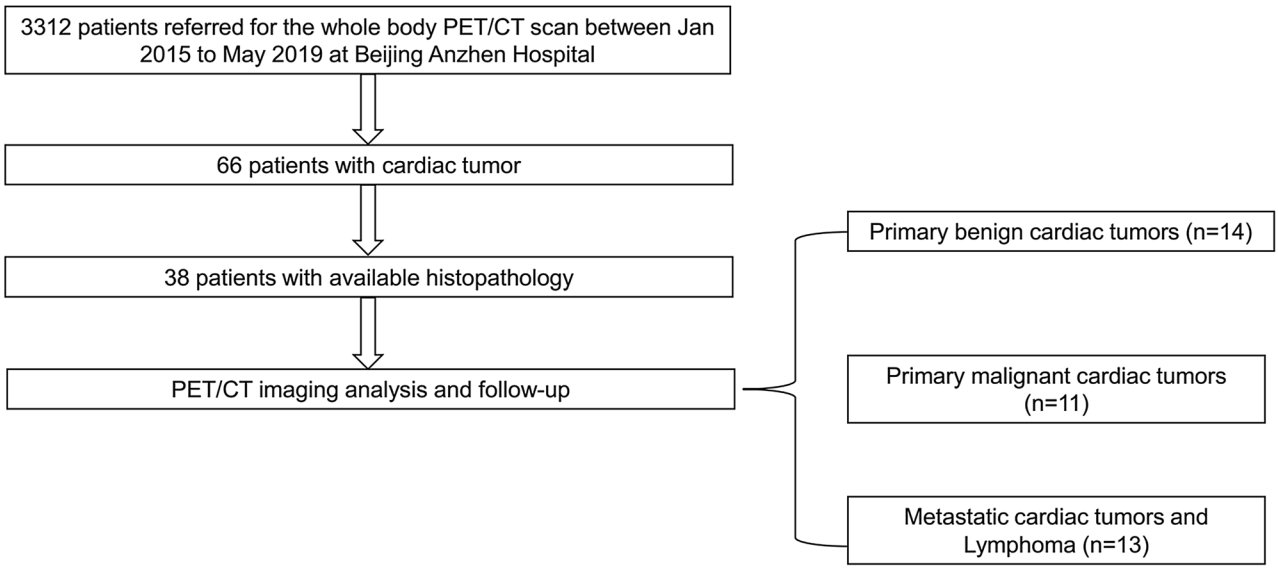

Figure 1. Patients flowchart.

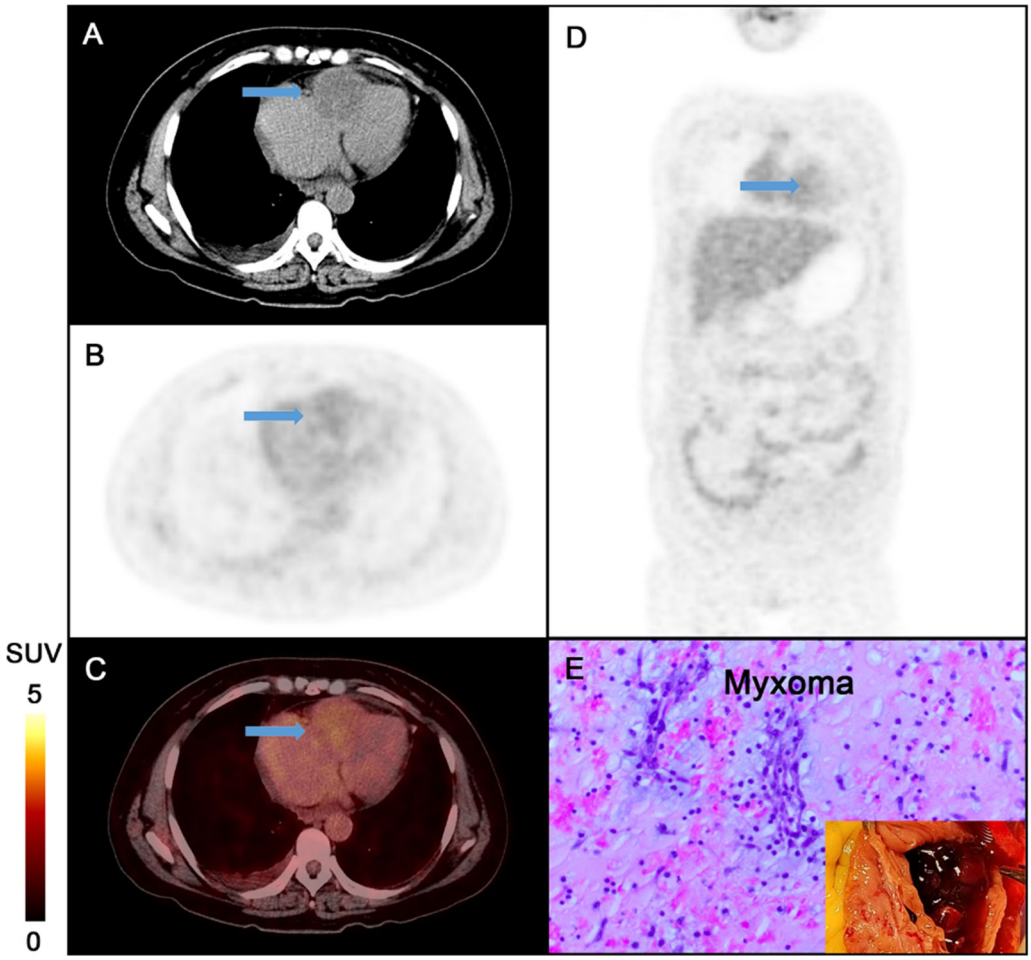

Figure 2. 44-year-old female presenting with dyspnea, abdominal distention, and lower extremity edema for 6 months. **A**, **B**, **C**: Transverse views of CT, PET, and PET/CT fusion. **D**: coronal view of PET. The blue arrow indicates the cardiac tumor. On CT, the right ventricle (RV) mass appears isodense or hypodense relative to the myocardium. ^{18}F-FDG PET shows mildly increased uptake in RV lesion (SUV_{max} 3.90, TBR_{max} 1.45): **E**: Intraoperative image of the tumor and histopathology, which revealed a primary cardiac myxoma (hematoxylin and eosin [HE] staining magnified 200 times).

groups by 1-way ANOVA followed by the Scheffe post hoc test. Categorical data are reported as percentages. Via receiver-operating characteristic (ROC) curve analysis, we determined the optimal SUV_{max} and TBR_{max} cut-off values to differentiate benign versus malignant cardiac tumors based on histology results as the gold standard. Sensitivity, specificity, accuracy, and area-under-the-curve (AUC) were calculated by χ^2 testing. Pearson correlation analysis was used to assess a relationship between tumor size and SUV_{max}. Kaplan–Meier survival curves were generated in subgroups classified using SUV_{max} and TBR_{max} cut-off values and were compared by log-rank test. The Cox proportional hazards regression analysis model was used to identify independent predictors of all-cause mortality in patients with cardiac lesions (n = 38). In the model, significant predictors were chosen via a stepwise forward method with $P < .05$ as the entry criterion and $P > .10$ as the removal criterion. Statistical significance was defined as $P < .05$.

RESULTS

Baseline characteristics of the patients with histological results (n = 38) are summarized in Table 1 and Supplemental data Table 1, respectively. Group 1, benign cardiac tumor (n = 14), was proven by surgery and histopathology. In Group 2, the primary malignant cardiac tumors (n = 11), only one case was verified by lung lesion biopsy; all others were confirmed by surgery and histopathology. In Group 3, cardiac metastasis and lymphoma were included (n = 13). Of 7 cases with DLBCL, two cases were diagnosed by extracardiac

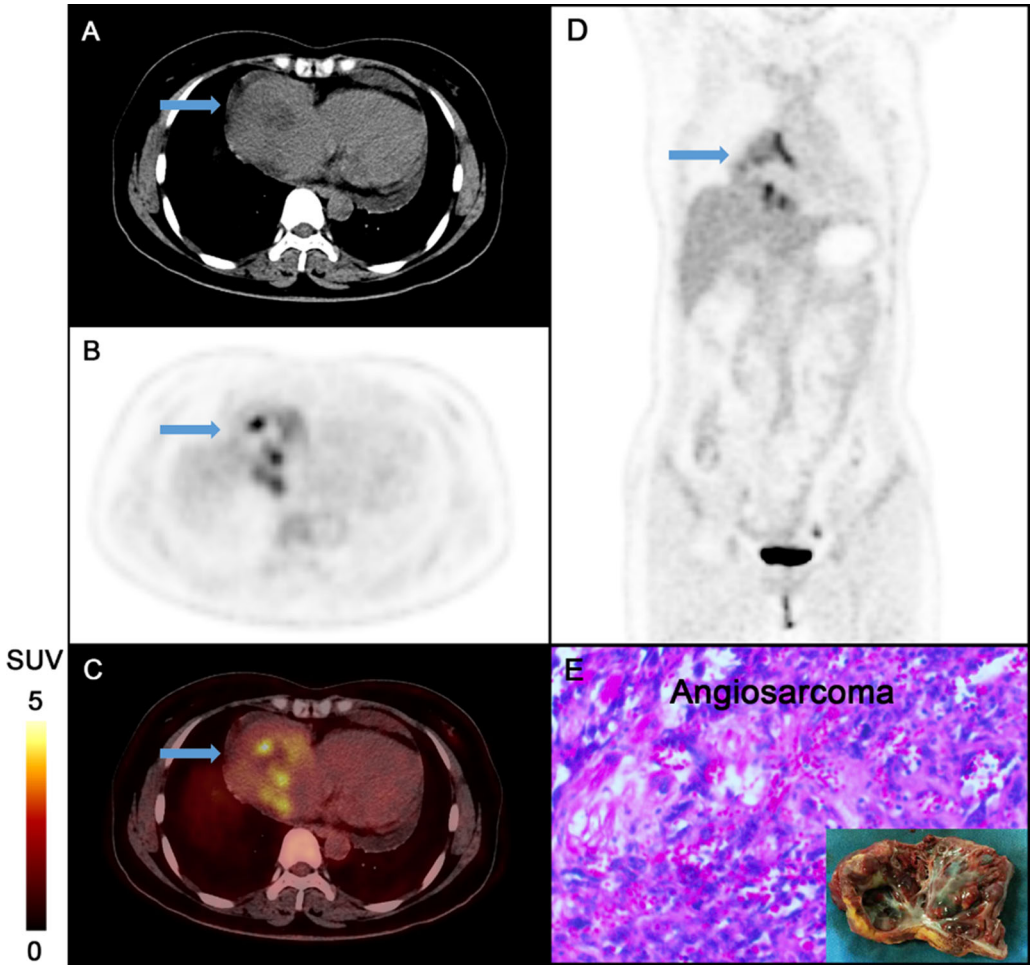

Figure 3. 47-year-old female presenting with palpitations and shortness of breath for 2 months. **A**, **B**, **C**: Transverse views of CT, PET, and PET/CT fusion. **D**: coronal view of PET. The blue arrow indicates the cardiac tumor. On CT, the right atrium (RA) masses appeared isodense or hypodense relative to the myocardium and a large pericardial effusion can be noted. ^{18}F-FDG PET/CT shows an increased uptake in this tumor (SUV_{max} 8.92; TBR_{max} 4.07). **E**: Gross biopsy specimen of the masses; histopathology revealed the lesion to be a primary angiosarcoma (HE staining magnified 200 times).

lesion biopsy (liver and bone). One patient was diagnosed by cardiac surgery and histopathology; the others were proved by lymph node biopsy. Four of the six patients with cardiac metastases were confirmed by extracardiac lesion biopsy (lung, bone, esophagus); two of them were verified by cardiac surgery and histopathology. All of the biopsied lesions were positive on PET.

Tumor Types and ^{18}F-FDG Uptake

As shown in Table 1, 14 (36.8%) of the patients presented with primary benign cardiac lesions were all verified histologically by surgery (Group 1, mean SUV_{max} = 2.35 ± 1.31, mean TBR_{max} = 1.05 ± 0.50), eleven patients (28.9%) had primary malignant cardiac tumors (Group 2, mean SUV_{max} = 8.90 ± 4.23, mean TBR_{max} = 3.82 ± 1.44), and 13 patients (34.2%) with cardiac metastases or lymphoma (Group 3, mean SUV_{max} = 14.37 ± 8.05, mean TBR_{max} = 6.19 ± 3.38).

A significant difference was observed in both SUV_{max} ($P < .001$) and TBR_{max} ($P < .001$) among three groups. Both mean SUV_{max} ($P < .001$) and mean TBR_{max} ($P < .001$) were significantly lower in Group 1 than those in Group 3. Moreover, both mean SUV_{max} ($P < .05$) and mean TBR_{max} ($P < .05$) in Group 1 were significantly lower than those in Group 2. TBR_{max} were significantly lower in Group 2 than that in Group 3

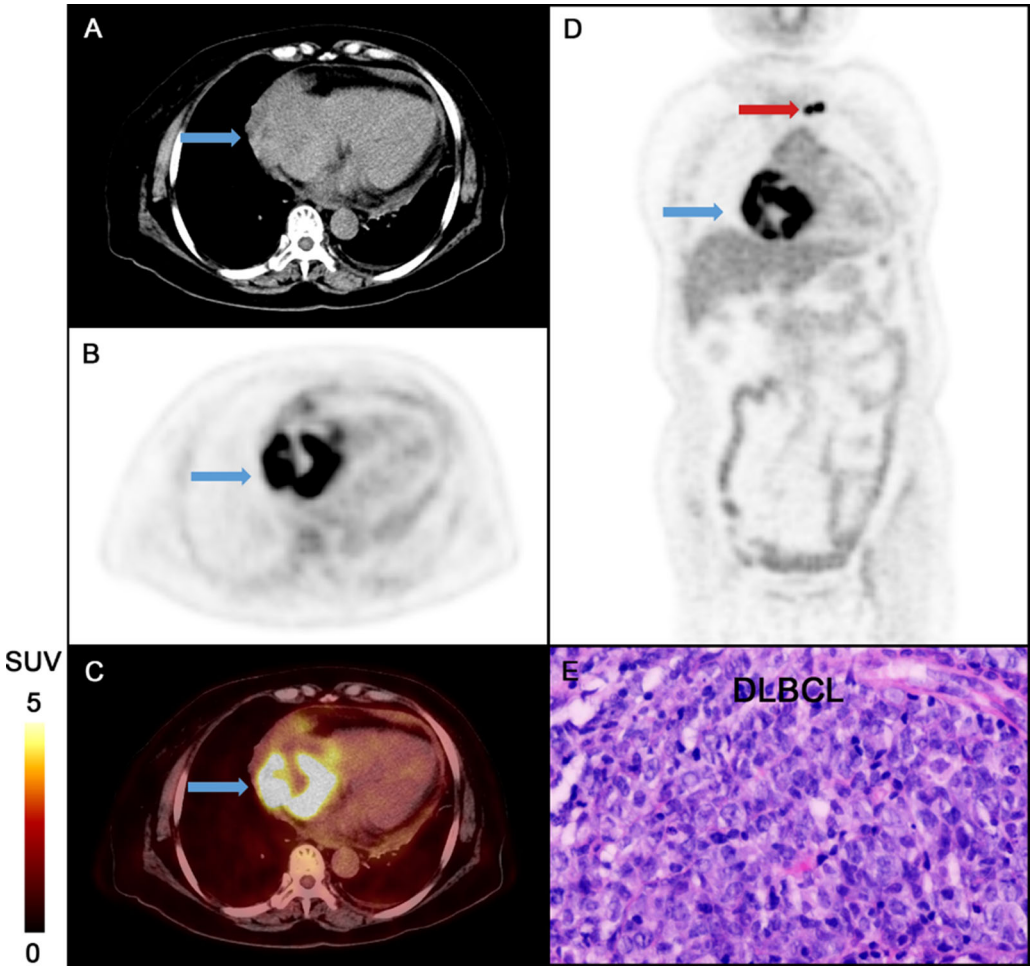

Figure 4. 73-year-old female presenting with increasing dyspnea for 2 years. **A**, **B**, **C**: Transverse views of CT, PET, and PET/CT fusion. **D**: Coronal view of PET. The blue arrow indicates the cardiac tumor, the red arrow increased uptake in lymph node manifestations. On CT scan, the RA masses appear isodense or hypodense relative to the myocardium. ^{18}F-FDG PET/CT depicts distinctly increased uptake in the RA tumor (SUV_{max} 21.00; TBR_{max} 8.47). **E**: Histopathology revealed the tumor to be DLBCL (HE staining magnified 200 times).

($P < .05$). Pearson correlation analysis showed a significant correlation between tumor size and SUV_{max} ($R^2 = 0.44$, $P = .006$) and a significant difference of the size of tumor between the benign and malignant tumors was observed ($P = .04$).

Among these 38 patients, 5 myxoma patients (all female, range of age 18-52) presented with a considerable variability of ^{18}F-FDG uptake (mean $SUV_{max} = 3.31 \pm 1.21$, range 1.91-5.23 and mean $TBR_{max} = 1.45 \pm 0.37$, range 1.00-2.02). In 10 cases of different types of sarcoma, the mean SUV_{max} is 8.20 ± 3.73 (ranging 3.80-14.37) and the mean TBR_{max} is 3.57 ± 1.26 (ranging 1.61-5.50), were calculated; 2 patients had bilateral pulmonary metastases.

Remarkably, a very high ^{18}F-FDG uptake (mean $SUV_{max} = 19.66 \pm 6.05$, range 13.61-31.60; mean $TBR_{max} = 8.46 \pm 2.56$, range 5.25-12.85) was observed in 7 patients with histologically confirmed as cardiac involvement of diffuse large B-cell lymphoma (DLBCL). The SUV_{max} in patients with DLBCL was significantly higher than the other malignant tumors (including primary malignant and metastatic cardiac tumors) (n = 17, mean $SUV_{max} = 8.79 \pm 4.31$, range 3.49-18.12; mean $TBR_{max} = 3.72 \pm 1.59$, range 1.27-7.05, $P < .05$).

Table 1. Characteristics of the three groups of patients

	Group 1 (n = 14)	Group 2 (n = 11)	Group 3 (n = 13)	*P* value
Age	45 ± 12	44 ± 11	59 ± 13	.004
Female/male	12/2	6/5	4/9	.015
SUV_{max}	2.35 ± 1.31*†	8.90 ± 4.23	14.37 ± 8.05	.001
TBR_{max}	1.05 ± 0.50*†	3.82 ± 1.44‡	6.19 ± 3.38	.001
Size(cm)	4.2 ± 1.4	6.0 ± 2.2	5.8 ± 3.4	.122
Treatment strategy				
Surgical resection	100%(14)	72.7%(8)	7.7%(1)	.001
Chemotherapy	-	9.0%(1)	69.2%(9)	
Surgical resection + chemotherapy	-	18.2%(2)	15.4%(2)	
No treatment	-	-	1	
Survival	92.9%(13)	45.5%(5)	53.8%(7)	.025

*$P < .05$ vs Group 2
†$P < .001$ vs Group 3
‡$P < .05$ vs Group 3

SUV_{max} and TBR_{max} CUT-OFFS

Table 2 shows the diagnostic performance for the differentiation of benign vs malignant using these cut-off values for SUV_{max} and TBR_{max}. According to ROC curve analysis, the optimal cut-offs to differentiate benign and malignant (primary and metastatic) cardiac lesions were a SUV_{max} of 3.44 with AUC = 0.988, $P < .001$, and a TBR_{max} of 1.55 with AUC = 0.979, $P < .001$. Using a best discriminative SUV_{max} cut-off of 3.44 for the cardiac tumors, the sensitivity, specificity, and accuracy of ^{18}F-FDG PET/CT for identification of malignancy were 100% (24/24), 92.9% (13/14), and 97.4% (37/38), respectively. Additionally, the TBR_{max} cut-off value of 1.55 proved to be equally suitable in detecting malignancy with a sensitivity of 95.8% (23/24), a specificity of 92.9% (13/14), and the diagnostic accuracy of 94.7% (36/38), respectively.

Survival

As shown in Figure 5, Kaplan–Meier cumulative overall survival curves of three groups differed significantly ($P < .05$). Malignant tumors as categorized by $SUV_{max} \geq 3.44$ or $TBR_{max} \geq 1.55$ was associated with significantly higher mortality as compared to benign tumors with $SUV_{max} < 3.44$ or $TBR_{max} < 1.55$ ($P = .018$ and $P = .002$, respectively) (Figure 6). All benign patients underwent surgery. Yet, there were different treatment methods for malignant patients. The Kaplan–Meier survival curve showed a significant difference with different treatment methods among patients with malignant cardiac tumors (Log rank 14.997, $P = .002$) (Figure 7).

COX Regression Analysis

As shown in Table 3, univariate Cox regression analysis revealed that the lesion dignity as determined by the cut-off value of SUV_{max} (HR 95% CI 7.834 [1.016-60.411], $P = .048$) was an independent predictor for death in patients with cardiac tumors, so was the pathological diagnosis (HR 95% CI 9.275 [1.201-71.645], $P = .033$). The other variables, including age, gender, tumor location, size, and treatment strategy had no independent predictive value for mortality.

DISCUSSION

To date, literature regarding cardiac tumors evaluated by ^{18}F-FDG PET/CT is scarce.[14-16,18] In our current study, so far with a largest number of patients, we assessed the ability of ^{18}F-FDG PET/CT imaging to determine cardiac tumor dignity. The diagnostic value of ^{18}F-FDG PET/CT was validated by histopathology. Additionally, the PET imaging characteristics of primary benign, primary malignant, and metastatic cardiac lesions were assessed and survival was also evaluated.

In this study, ^{18}F-FDG PET/CT showed excellent diagnostic performance in differentiating benign from malignant cardiac tumors. Cut-off values obtained for both measures of ^{18}F-FDG uptake, SUV_{max} and TBR_{max}, resulted in very good sensitivity, specificity, and

Table 2. Performance of SUV_{max} and TBR_{max} cut-offs in distinguishing benign versus malignant cardiac tumors (n = 38)

Uptake variable (cut-off value for malignancy)	Sensitivity, % (n = 24)	Specificity, % (n = 14)	Accuracy, % (n = 38)	AUC	*P* value
SUV_{max} (≥ 3.44)	100 (24/24)	92.9 (13/14)	97.4 (37/38)	0.988	< .001
TBR_{max} (≥ 1.55)	95.8 (23/24)	92.9 (13/14)	94.7 (36/38)	0.979	< .001

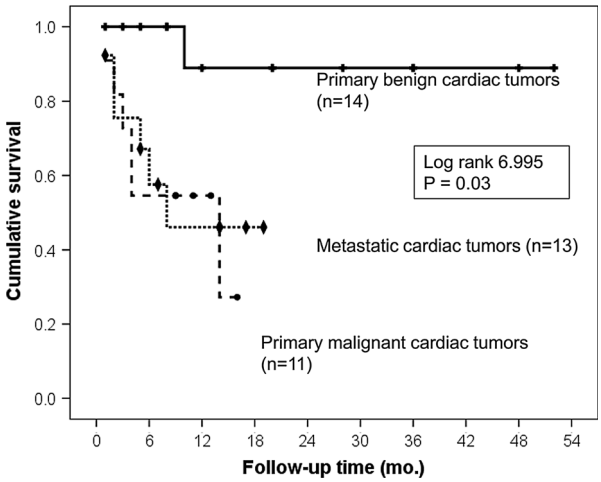

Figure 5. Kaplan–Meier cumulative overall survival curves of 38 patients categorized into three groups, Group 1 with primary cardiac tumors (n = 14), Group 2 with primary malignant cardiac tumors (n = 11), and Group 3 with cardiac metastases and lymphoma (n = 13) (log rank 6.995, *P* = .030).

accuracy. Our observations aligned well with those of the previous studies in smaller patient populations,[14,15] as well as those of the only study yet published using ^{18}F-FDG PET/MR.[19] Our SUV_{max} cut-off of 3.44 is well consistent with the SUV_{max} cut-off of 3.5 obtained by Rabhar et al [14] and SUV_{max} cut-off of 3.5-4.0 by Shao et al.[15]

In contrast to the previous studies,[14,15,19] we also investigated a second variable of ^{18}F-FDG uptake, the TBR_{max}. This variable was calculated using a reference VOI in the liver, because hepatic ^{18}F-FDG uptake has been shown to correlate with circulating ^{18}F-FDG levels,[20] and the liver's size makes it easy to assign VOIs. Additionally, TBR_{max} appears to be less influenced by, for e.g., body composition, presumably also image reconstruction methods or PET equipment, as compared to SUV_{max}.[21-24] Remarkably, TBR_{max} at the calculated optimal cut-off, 1.55, proved to have similar diagnostic accuracy as the calculated optimal SUV_{max} cut-off of 3.44.

As another main finding, our analysis suggested that in patients with cardiac tumors, ^{18}F-FDG PET/CT was able to detect suspicious hypermetabolic extracardiac lesions, and hence may be a valuable staging tool in this setting. In our study, 2 patients with primary cardiac malignancy were found to have bilateral lung metastases and 13 had lesions of non-cardiac origin, including 7 cases of DLBCL. The ability to identify extracardiac lesions potentially has a significant impact on patient management. On one hand, better visualization and localization of lesions facilitate histological verification of cancer. On the other hand, such findings may render cardiac surgery obsolete in many cases, allowing patients to be switched to other treatment modalities that may be more appropriate for their disease, e.g., chemotherapy or targeted therapy (shown in Supplemental data, Table 1). This is especially the case for lymphoma involving the heart where surgery usually is contraindicated. Our analysis showed prominently increased cardiac ^{18}F-FDG activity (SUV_{max} and TBR_{max}) in 7 patients with cardiac DLBCL, 6 lesions localized in the right heart. The imaging pattern could be recognized and distinguished from other malignant cardiac tumors.

Differentiating primary from metastatic malignant heart lesions is another significant clinical challenge. According to our results, ^{18}F-FDG uptake (TBR_{max}) in primary malignant cardiac tumor is lower than metastases to the heart or lymphoma. This finding might contribute to a better discrimination in clinical unclear constellations.

Finally, and importantly, our study results indicated that ^{18}F-FDG uptake was a useful prognostic variable in patients with histological diagnosis. Kaplan–Meier cumulative overall survival curves showed that patient with malignant tumors categorized by $SUV_{max} \geq 3.44$ or $TBR_{max} \geq 1.55$ was associated with significantly higher mortality as compared to benign tumors (*P* = .018 and

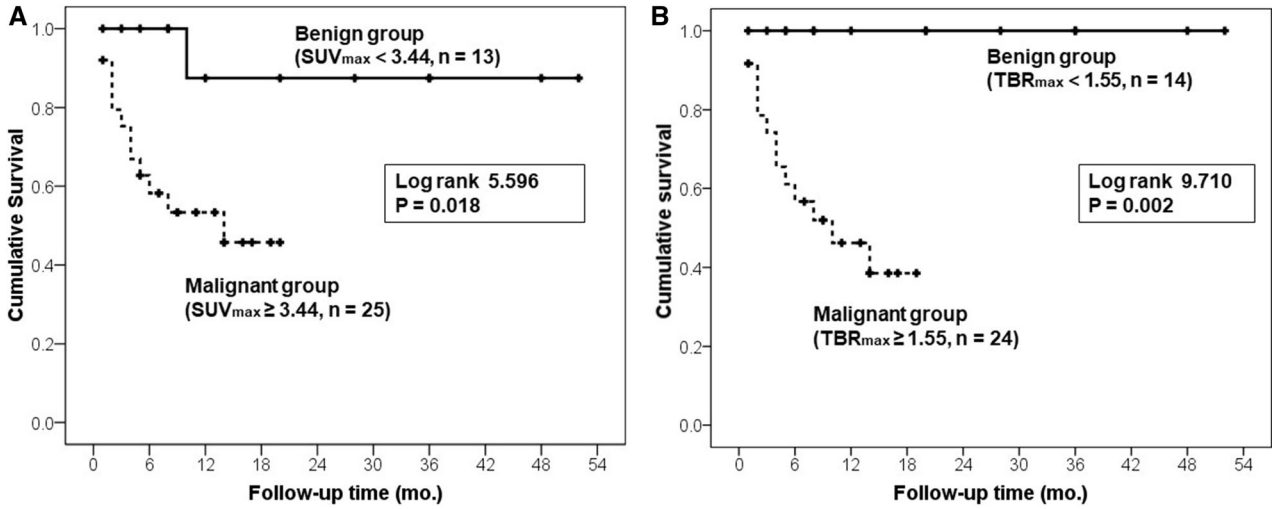

Figure 6. Kaplan–Meier cumulative survival curves of patients with cardiac tumors (n = 38) classified by SUV_{max} and TBR_{max} using the calculated optimal cut-off values. **A**: Estimated overall survival was significantly lower in the malignant group ($SUV_{max} \geq 3.44$, n = 25) than in the benign group ($SUV_{max} < 3.44$, n = 13) (log rank 5.596, $P = .018$). **B**: Similarly, estimated overall survival was significantly lower in the malignant group ($TBR_{max} \geq 1.55$, n = 24) than in the benign group ($TBR_{max} < 1.55$, n = 14) log rank 9.710, $P = .002$).

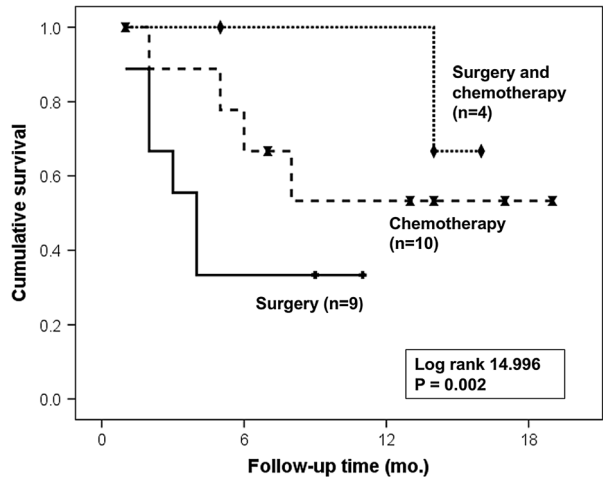

Figure 7. Kaplan–Meier cumulative survival curves in 23 patients with malignant cardiac tumors using different treatment strategies (log rank 14.996, $P = .002$).

$P = .002$, respectively). On the Cox regression analysis using relevant variables, including age, gender, tumor size, tumor location, treatment strategy, tumor dignity as determined by the cut-off values of SUV_{max} 3.44 and the tumor dignity by histopathology, only the cut-off value of SUV_{max} 3.44 and histopathological diagnosis were independent predictors for death, which has not been previously reported.

LIMITATIONS

This was a single-center study of a Chinese expert center cohort with a wide variety of cardiac and other tumor types, and thus the generalizability of our findings may be limited. Also raising potential issues of generalizability, the prevalence of benign lesions, of certain tumor types, and of certain sites of cardiac tumor in our patients differed from those in other published series. For example, frequency of angiosarcoma in our collective was lower than that reported frequency elsewhere,[25] as was the prevalence of right [26] or left atrial tumors.[27] Another notable difference between our work and earlier work is the substantially higher rate of cases of lymphoma in our sample.[27] These differences in disease characteristics may be attributable to either or both of center-specific selection biases, or ethnic composition of the respective cohorts. Finally, our study had a relatively short follow-up. Nonetheless, high mortality was observed (34.2%, 13/38), suggesting a poor prognosis for patients with cardiac tumors and the need for prompt diagnosis and treatment.

NEW KNOWLEDGE GAINED

FDG-PET/CT should be performed for the assessment of cardiac tumors; it also appears to be valuable for prognostication.

Table 3. Independent predictors of death by Cox Univariate and Multivariate Analyses in patients with cardiac tumors (n = 38)

	Univariate analysis		Multivariate analysis	
Variable	**Hazard ratio (95%CI)**	***P* value**	**Hazard Ratio (95%CI)**	***P* value**
Age	1.027 (0.980–1.077)	.263		
Gender	0.878 (0.294–2.626)	.816		
Size of tumor	0.998 (0.998–1.020)	.826		
Disease course	0.927(0.845–1.017)	.108		
Location in RA	0.893(0.291–2.739)	.844		
No metastatic lesion	0.432(0.144–1.293)	.133		
Treatment strategy	0.944(0.499–1.784)	.859		
SUV_{max} (Cut-off 3.44)	7.834 (1.016–60.411)	.048	7.834 (1.016–60.411)	.048
Pathological diagnosis	9.275(1.201–71.645)	.033		

CONCLUSION

^{18}F-FDG PET/CT, because of its high accuracy in determining, whether lesions are benign or malignant, should be included in the diagnostic algorithm for cardiac tumors. ^{18}F-FDG uptake, independently predicted survival in cardiac tumors and might serve as a valuable predictive tool for individualized decision-making.

Disclosure

The authors have indicated that they have no financial conflict of interest.

References

1. Elbardissi AW, Dearani JA, Daly RC, Mullany CJ, Orszulak TA, Puga FJ, et al. Survival after resection of primary cardiac tumors: A 48-year experience. Circulation 2008;118:S7-15.
2. Chiles C, Woodard PK, Gutierrez FR, Link KM. Metastatic involvement of the heart and pericardium: CT and MR imaging. Radiographics 2001;21:439-49.
3. Reynen K. Cardiac myxomas. N Engl J Med 1995;333:1610-7.
4. Bussani R, De-Giorgio F, Abbate A, Silvestri F. Cardiac metastases. J Clin Pathol 2007;60:27-34.
5. Hoffmeier A, Sindermann JR, Scheld HH, Martens S. Cardiac tumors–diagnosis and surgical treatment. Dtsch Arztebl Int 2014;111:205-11.
6. Donisan T, Balanescu DV, Lopez-Mattei JC, Kim P, Leja MJ, Banchs J, et al. In search of a less invasive approach to cardiac tumor diagnosis: Multimodality imaging assessment and biopsy. JACC Cardiovasc Imaging 2018;11:1191-5.
7. Grebenc ML, Rosado de Christenson ML, Burke AP, Green CE, Galvin JR. Primary cardiac and pericardial neoplasms: Radiologic-pathologic correlation. Radiographics 2000;20:1073-103; quiz 110-1, 112.
8. Mousavi N, Cheezum MK, Aghayev A, Padera R, Vita T, Steigner M, et al. Assessment of cardiac masses by cardiac magnetic resonance imaging: Histological correlation and clinical outcomes. J Am Heart Assoc 2019;8:e007829.
9. Barrington SF, Johnson PWM. (18)F-FDG PET/CT in lymphoma: Has imaging-directed personalized medicine become a reality? J Nucl Med 2017;58:1539-44.
10. Laurens ST, Oyen WJ. Impact of fluorodeoxyglucose PET/computed tomography on the management of patients with colorectal cancer. PET Clin 2015;10:345-60.
11. Ciarallo A, Marcus C, Taghipour M, Subramaniam RM. Value of fluorodeoxyglucose PET/computed tomography patient management and outcomes in thyroid cancer. PET Clin 2015;10:265-78.
12. Werner RA, Schmid JS, Higuchi T, Javadi MS, Rowe SP, Markl B, et al. Predictive value of (18)F-FDG PET in patients with advanced medullary thyroid carcinoma treated with vandetanib. J Nucl Med 2018;59:756-61.
13. Weber WA. Positron emission tomography as an imaging biomarker. J Clin Oncol 2006;24:3282-92.
14. Rahbar K, Seifarth H, Schafers M, Stegger L, Hoffmeier A, Spieker T, et al. Differentiation of malignant and benign cardiac tumors using 18F-FDG PET/CT. J Nucl Med 2012;53:856-63.
15. Shao D, Wang SX, Liang CH, Gao Q. Differentiation of malignant from benign heart and pericardial lesions using positron emission tomography and computed tomography. J Nucl Cardiol 2011;18:668-77.
16. Masuda A, Manabe O, Oyama-Manabe N, Naya M, Obara M, Sakakibara M, et al. Cardiac fibroma with high (18)F-FDG uptake mimicking malignant tumor. J Nucl Cardiol 2017;24:323-4.
17. Burke A, Tavora F. The 2015 WHO classification of tumors of the heart and pericardium. J Thorac Oncol.
18. Rinuncini M, Zuin M, Scaranello F, Fejzo M, Rampin L, Rubello D, et al. Differentiation of cardiac thrombus from cardiac tumor combining cardiac MRI and 18F-FDG-PET/CT Imaging. Int J Cardiol 2016;212:94-6.
19. Nensa F, Tezgah E, Poeppel TD, Jensen CJ, Schelhorn J, Kohler J, et al. Integrated 18F-FDG PET/MR imaging in the assessment of cardiac masses: A pilot study. J Nucl Med 2015;56:255-60.
20. Liu G, Hu Y, Zhao Y, Yu H, Hu P, Shi H. Variations of the liver standardized uptake value in relation to background blood metabolism: An 2-[18F]Fluoro-2-deoxy-D-glucose positron emission

tomography/computed tomography study in a large population from China. Medicine (Baltimore) 2018;97:e0699.
21. Li X, Samnick S, Lapa C, Israel I, Buck AK, Kreissl MC, et al. 68Ga-DOTATATE PET/CT for the detection of inflammation of large arteries: Correlation with18F-FDG, calcium burden and risk factors. EJNMMI Res 2012;2:52.
22. Dunet V, Halkic N, Prior JO, Anaye A, Meuli RA, Sempoux C, et al. Detection and viability of colorectal liver metastases after neoadjuvant chemotherapy: A multiparametric PET/CT-MRI study. Clin Nucl Med 2017;42:258-63.
23. Ezziddin S, Adler L, Sabet A, Poppel TD, Grabellus F, Yuce A, et al. Prognostic stratification of metastatic gastroenteropancreatic neuroendocrine neoplasms by 18F-FDG PET: Feasibility of a metabolic grading system. J Nucl Med 2014;55:1260-6.
24. Sharma A, Mohan A, Bhalla AS, Vishnubhatla S, Pandey AK, Bal CS, et al. Role of various semiquantitative parameters of 18F-FDG PET/CT studies for interim treatment response evaluation in non-small-cell lung cancer. Nucl Med Commun 2017;38:858-67.
25. Pun SC, Plodkowski A, Matasar MJ, Lakhman Y, Halpenny DF, Gupta D et al. Pattern and prognostic implications of cardiac metastases among patients with advanced systemic cancer assessed with cardiac magnetic resonance imaging. J Am Heart Assoc 2016;5.
26. Dhull VS, Sharma P, Mukherjee A, Jana M, Bal C, Kumar R. 18F-FDG PET-CT for evaluation of cardiac angiosarcoma: A case report and review of literature. Mol Imaging Radionucl Ther 2015;24:32-6.
27. Mkalaluh S, Szczechowicz M, Torabi S, Schmack B, Sabashnikov A, Dib B, et al. Surgical treatment of cardiac tumors: Insights from an 18-year single-center analysis. Med Sci Monit 2017;23:6201-9.